AIP Applied Physics Letters

Continuous and unconstrained manipulation of micro-particles using phase-control of bulk acoustic waves

J. Greenhall, F. Guevara Vasquez, and B. Raeymaekers

Citation: Applied Physics Letters **103**, 074103 (2013); doi: 10.1063/1.4819031
View online: http://dx.doi.org/10.1063/1.4819031
View Table of Contents: http://scitation.aip.org/content/aip/journal/apl/103/7?ver=pdfcov
Published by the AIP Publishing

Articles you may be interested in

Phase-control of a rising sun magnetron using a modulated, addressable, current source
J. Vac. Sci. Technol. B **33**, 031203 (2015); 10.1116/1.4916631

Intrinsically tunable 0.67BiFeO3-0.33BaTiO3 thin film bulk acoustic wave resonators
Appl. Phys. Lett. **101**, 232903 (2012); 10.1063/1.4769346

Efficient counter-propagating wave acoustic micro-particle manipulation
Appl. Phys. Lett. **101**, 233501 (2012); 10.1063/1.4769092

Quantitative trap and long range transportation of micro-particles by using phase controllable acoustic wave
J. Appl. Phys. **112**, 054908 (2012); 10.1063/1.4751022

Manipulation of microparticles using phase-controllable ultrasonic standing waves
J. Acoust. Soc. Am. **128**, EL195 (2010); 10.1121/1.3479976

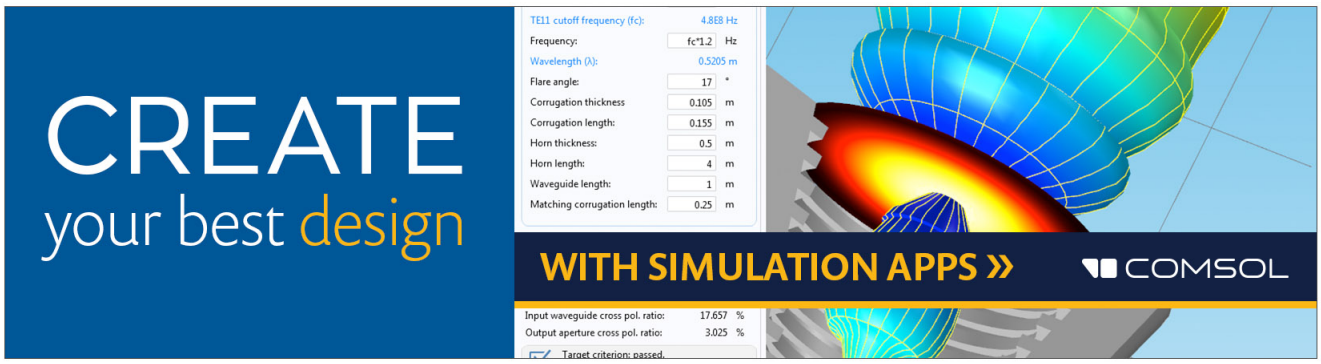

This article is copyrighted as indicated in the article. Reuse of AIP content is subject to the terms at: http://scitation.aip.org/termsconditions. Downloaded to IP: 155.101.97.169 On: Fri, 15 May 2015 20:50:59

Continuous and unconstrained manipulation of micro-particles using phase-control of bulk acoustic waves

J. Greenhall,[1] F. Guevara Vasquez,[2] and B. Raeymaekers[1,a)]
[1]*Department of Mechanical Engineering, University of Utah, Salt Lake City, Utah 84112, USA*
[2]*Department of Mathematics, University of Utah, Salt Lake City, Utah 84112, USA*

(Received 10 June 2013; accepted 7 August 2013; published online 15 August 2013)

A method of unconstrained and continuous manipulation of micro-particles in a fluid using bulk acoustic waves is theoretically derived and experimentally demonstrated. The method is based on phase-control of standing pressure waves created by two opposing transducers. Reflections are taken into account, removing the need for complex experiments. The operating domain of this method is characterized and compared to existing techniques. In contrast to methods based on linearly adjusting the phase difference between opposing transducers, it is shown that by independently controlling the phase of each transducer, particles can be manipulated in an unconstrained manner over multiple wavelengths. © *2013 AIP Publishing LLC*.
[http://dx.doi.org/10.1063/1.4819031]

Precise control and manipulation of particles dispersed in a host fluid contained in a reservoir is of critical importance for applications in biology,[1] biomedical devices,[2] process control,[3] and directed self-assembly of nano- and micro-particles,[4] amongst others. Manipulation of particles using acoustic waves can be achieved in two regimes. If the particle diameter, D, is much larger than the wavelength, λ, of the acoustic wave, intensity gradients arising from refraction drive particles to the intensity wells (ray acoustics regime). This is oftentimes referred to as acoustic tweezers.[5,6] Conversely, if $D \ll \lambda$, the acoustic radiation force associated with the pressure wave manipulates particles dispersed in a host fluid to the nodes or antinodes of this wave[7] (Rayleigh regime). The acoustic contrast factor, $\Phi = (5\rho_p - 2\rho_f)/(2\rho_p + \rho_f) - \beta_p/\beta_f$, determines whether particles accumulate at the nodes ($\Phi > 0$) or antinodes ($\Phi < 0$) of the standing pressure wave. Here, ρ_p, ρ_f, β_p, and β_f are the density and compressibility of the particles and the host fluid, respectively.[8] Controlling the position of the nodes enables manipulation of particles trapped in the nodes to a predetermined location in the host fluid reservoir. This is commonly achieved through use of transducer arrays.[9–13] In this paper, we focus on the phase adjustable transducer array technique with counter-propagating wave patterns.[11–13] Courtney *et al.*[12,13] used opposing piezoelectric transducers (PZT) operating near 5 MHz to create counter propagating pressure waves in water. Matching and backing layers were attached to the transducers to absorb incoming waves and reduce reflections. Using the phase difference between the two transducers, in the absence of reflections, they state that particles can be displaced across multiple wavelengths, and experimental data shows displacement of particles over a half wavelength. This method requires precise implementation of the backing and matching layers to suppress reflected waves. Grinenko *et al.*[14] alleviated this problem by backing the piezoelectric transducers with a fluid layer and then an acoustic absorbing layer. Alternatively, Kozuka *et al.*[11] employed two transducers arranged at 150° and operated at 39.6 kHz to generate a standing wave in air without reflections. They manipulated a 3 mm polystyrene (PS) sphere trapped in the antinode of the pressure wave, and showed that the sphere moved almost linearly with increasing phase difference between the two transducers.

The methods described in the literature to manipulate particles trapped in the nodes of a standing pressure wave are derived under the assumption that no reflected waves normal to the transducer surface exist. This results in a straightforward solution of the wave equation, but it also requires removing those reflections in practical implementations, either by creating a backing or acoustic absorption layer, or by arranging the transducers in an inclined orientation. Furthermore, no explicit demonstration seems to exist of manipulating a particle over multiple wavelengths using bulk acoustic waves (including reflections). This paper attempts to describe an alternative method, based on a solution of the wave equation that incorporates reflected waves, thus avoiding the need for complex practical implementations. The method requires independent adjustment of the phases of two opposing transducers, and enables unconstrained, continuous manipulation of particles dispersed in a host fluid over multiple wavelengths, in the presence of reflected waves. A theoretical analysis and experimental validation is presented.

Figure 1 shows the cross-section of a fluid reservoir of length L with two opposing transducers. The pressure (acoustic) wave, $p(x, t)$, generated by the transducers is described by the one-dimensional (1D) inviscid wave equation.[15] Because the pressure field in the reservoir consists of standing waves, it can be reduced to the time independent Helmholtz equation[16]

$$\frac{\partial^2 p}{\partial x^2} + k^2 p = 0, \tag{1}$$

where x is the direction of wave propagation, $p(x)$ is the pressure, and k is the wave number. Assuming rigid transducer

a)Electronic mail: bart.raeymaekers@utah.edu

 © 2013 AIP Publishing LLC

This article is copyrighted as indicated in the article. Reuse of AIP content is subject to the terms at: http://scitation.aip.org/termsconditions. Downloaded to IP: 155.101.97.169 On: Fri, 15 May 2015 20:50:59

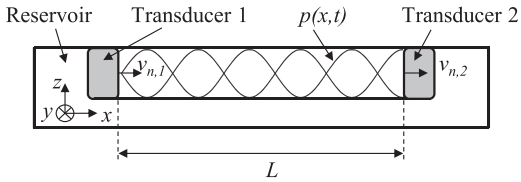

FIG. 1. Cross-sectional view of a fluid reservoir with two opposing transducers creating a standing pressure wave $p(x, t)$.

surfaces, the boundary condition at the fluid-transducer interface is derived from the continuity equation as

$$\vec{n} \cdot \nabla p = j\omega\rho_f v_{n,i}, \tag{2}$$

where $\vec{n}$ is the unit vector normal to the transducer surface (x-direction, see Fig. 1), ω is the transducer angular frequency, ρ_f is the fluid density, and $v_{n,i}$ is the velocity of the surface of transducer i (with $i \in \{1, 2\}$) in the positive x-direction, given as

$$\begin{aligned} v_{n,1} &= A_1 e^{j\psi_1} \quad \text{at } x = 0 \quad \text{and} \\ v_{n,2} &= A_2 e^{j\psi_2} \quad \text{at } x = L. \end{aligned} \tag{3}$$

A_1 and A_2 are the velocity amplitudes, and ψ_1 and ψ_2 are the phases of the oscillating transducer surfaces. In this paper, $A_1/A_2 = 1$. With these boundary conditions, the pressure of the standing wave as a function of location is calculated as

$$\begin{aligned} p(x) = \frac{\rho_f}{2k \sin kL} &(A_1 e^{j\psi_1}(e^{jk(x-L)} + e^{-jk(x-L)}) \\ &- A_2 e^{j\psi_2}(e^{jkx} + e^{-jkx})), \end{aligned} \tag{4}$$

the real part of which can be written as

$$\begin{aligned} \Re\mathrm{e}[p(x)] = \frac{\rho_f}{k \sin kL} &(A_1 \cos\psi_1 \cos(k(L-x)) \\ &- A_2 \cos\psi_2 \cos kx). \end{aligned} \tag{5}$$

The location of the nodes are computed as $\Re\mathrm{e}[p] = 0$, which yields

$$x(\psi_1, \psi_2) = \frac{1}{k}\,\mathrm{atan}\left(\frac{A_2 \cos\psi_2 - A_1 \cos\psi_1 \cos kL}{A_2 \cos\psi_1 \sin kL}\right) + \frac{m\pi}{k}. \tag{6}$$

Here, $m = [0, 1, 2, \ldots, n]$, so that all nodal locations are contained between 0 and L. n is the number of nodes of the standing pressure wave between the opposing transducers. When $k = (2n-1)\pi/2L$, for $n \in \mathbb{N}$, Eq. (6) is reduced to

$$x(\psi_1, \psi_2) = \frac{(-1)^{n+1}}{k}\,\mathrm{atan}\left(\frac{A_2 \cos\psi_2}{A_1 \cos\psi_1}\right) + \frac{m\pi}{k}. \tag{7}$$

Figure 2(a) shows the nodal locations ($x/\lambda \in [0, 3]$) of the standing pressure wave as a function of the phases of the opposing transducers, ψ_1 and ψ_2, for the case of Eq. (7), with $n = 48$. Only even values of m are displayed for clarity. The inset shows a section of Fig. 2(a) for $\psi_1, \psi_2 \in [0, \pi]$. Four example trajectories of a particle trapped in a node are

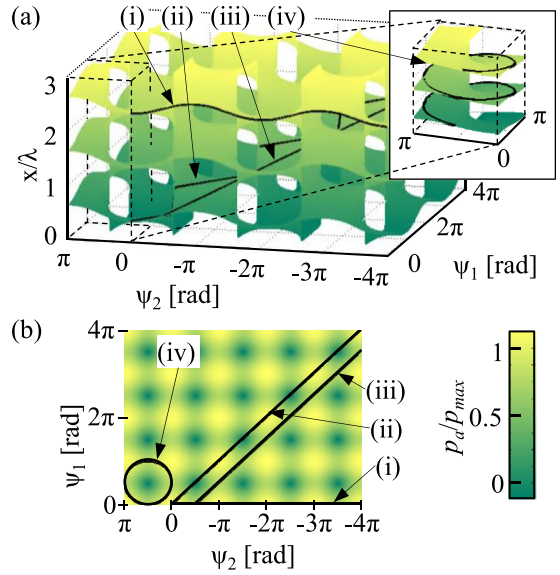

FIG. 2. (a) Nodal locations of the standing pressure wave, x/λ, as a function of the transducer phases, ψ_1 and ψ_2 (for even values of m). The inset shows the section of the figure boxed with dashed lines. Four example node trajectories are shown (solid line); trajectories (i) and (ii) are based on linear adjustments of $\Delta\psi(t)$, while trajectories (iii) and (iv) are based on independent adjustments of ψ_1 and ψ_2. (b) Amplitude of the standing pressure wave as a function of ψ_1 and ψ_2, identifying the same trajectories (i)–(iv) shown in (a) (solid lines), and illustrating that for certain combinations of ψ_1 and ψ_2, the amplitude of the standing pressure wave approaches zero (darker), eliminating the ability to control a particle trapped in a node.

indicated with a solid line. Trajectories (i) and (ii) are obtained by linearly adjusting the phase difference between the transducers, $\Delta\psi = \psi_1 - \psi_2$ (i.e., $\Delta\psi(t)$ follows a straight line and $\Delta\psi(0) = 0$). We observe that linear adjustment of $\Delta\psi$ will not result in displacement over multiple wavelengths. In contrast, trajectories (iii) and (iv) show that through simultaneous and independent adjustment of both transducer phases, a particle trapped in a node can be displaced over multiple wavelengths. We assume that the pressure satisfies the Helmholtz equation when the transducer phases are adjusted, i.e., the transient behavior is neglected. This is an adequate approximation if the changes in the transducer phases occur over a time scale that is significantly larger than the period of the pressure wave, as is the case in our experiments. While only four trajectories resulting from specific sequences of the transducer phases are identified, an infinite number of sequences theoretically exists (Fig. 2). Practically, however, particles cannot be trapped and manipulated unless the amplitude of the standing pressure wave, $p_a \neq 0$. Figure 2(b) shows the amplitude of the standing pressure wave, p_a, as a function of ψ_1 and ψ_2, normalized with the maximum possible pressure amplitude, p_{max}, for the given reservoir dimensions.

Figure 3 shows a schematic of the experimental apparatus. It consists of a reservoir (inner dimensions: 48×48×8 mm) machined from poly(methyl methacrylate). Two PZT transducers (type SM411) of dimensions (5×45×8 mm) and center frequency of 740 kHz are mounted on opposing walls of the reservoir. The transducers are driven by a function generator controlled by a personal computer (PC). A spherical polystyrene particle of diameter 350 μm is displaced

This article is copyrighted as indicated in the article. Reuse of AIP content is subject to the terms at: http://scitation.aip.org/termsconditions. Downloaded to IP: 155.101.97.169 On: Fri, 15 May 2015 20:50:59

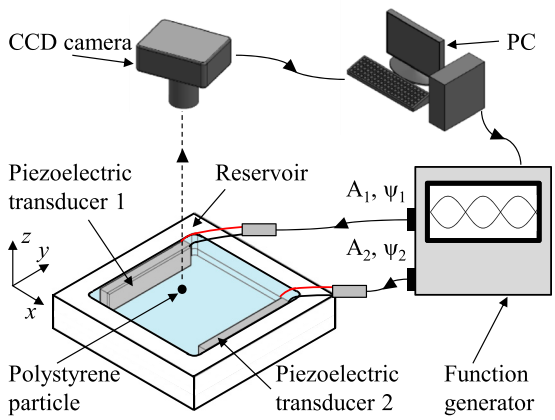

FIG. 3. Experimental setup consisting of a water reservoir with two opposing piezoelectric transducers. A spherical polystyrene particle of diameter 350 μm is neutrally buoyant in the reservoir. The transducer phases, ψ_1 and ψ_2, are adjusted by the function generator according to a specified sequence controlled by a PC, while $A_1/A_2 = 1$. The particle is manipulated along the x-direction of the reservoir, and its displacement is captured with a CCD camera. A particle tracking algorithm is employed to quantify its position during manipulation.

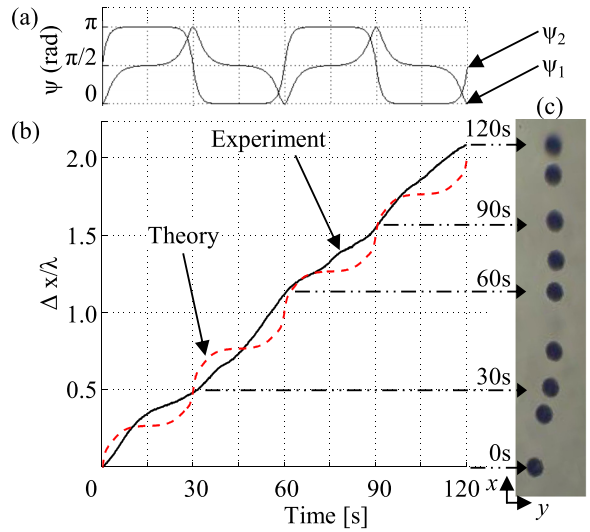

FIG. 4. Comparison of experimental and theoretical results. (a) The sequence of transducer phases, ψ_1 and ψ_2, as a function of time and (b) the corresponding theoretical and experimental displacement of a particle trapped in a node of the standing pressure wave. (c) A composite picture of snapshots in time of the particle as it traverses two wavelengths in the reservoir, demonstrating that the particle can be displaced multiple wavelengths by independently adjusting the phases of two opposing transducers.

along the x-direction of the reservoir over two wavelengths by applying a sequence of ψ_1 and ψ_2 to the respective transducers, as theoretically described by the solid line in the inset of Fig. 2(a) (trajectory (iv)). The position of the particle is captured with a CCD camera and its displacement is quantified using a particle tracking algorithm. The fluid host medium consists of deionized water mixed with sugar to render the particle neutrally buoyant in the fluid and keep it away from the reservoir walls. The density and sound speed are $\rho_p = 1062\,\mathrm{kg/m^3}$ (measured), $c_p = 2400\,\mathrm{m/s}$ (Ref. 17) for the PS particle and $\rho_f = 1062\,\mathrm{kg/m^3}$ (measured), $c_f = 1497\,\mathrm{m/s}$ (determined with time-of-flight measurement) for the fluid and, thus, the acoustic contrast factor $\Phi = 0.609$.

Figure 4 shows the experimental results, with (a) the sequence of transducer phases that result in trajectory (iv) shown in the inset of Fig. 2(a), (b) the theoretical (dashed) and experimental (solid) position of a particle trapped in a node of the standing pressure wave, as the node is displaced over two wavelengths by adjusting the phases as described in (a), and (c) shows a composite image made of snapshots in time of the particle as it traverses the two wavelength distance. This demonstrates experimentally that a particle can be manipulated over multiple wavelengths, when independently adjusting the transducer phases. The experiment closely matches the theoretical trajectory of a particle trapped in the node of the standing pressure wave, subject to the imposed sequence of ψ_1 and ψ_2. The slight difference between the theoretical and experimental particle displacement is likely the result of minute misalignment of the opposing transducers, which may alter the standing wave pattern due to reflections of the waves from the reservoir walls. Furthermore, inertia and viscous drag, not included in the model, prevent the particle from instantaneously tracking the displacement of the node of the standing pressure wave, upon changing the transducer phases. This results in a more continuous displacement of the particle than theoretically predicted.

Figures 5(a)–5(d) show the displacements, $\Delta x/\lambda$, resulting from the four example trajectories (i)–(iv) identified in Fig. 2, and displays the transducer phase sequences (left column) along with the corresponding displacements (solid line) and pressure amplitudes (dashed lines) of the standing pressure wave (right column). In Fig. 5(a), the linear change

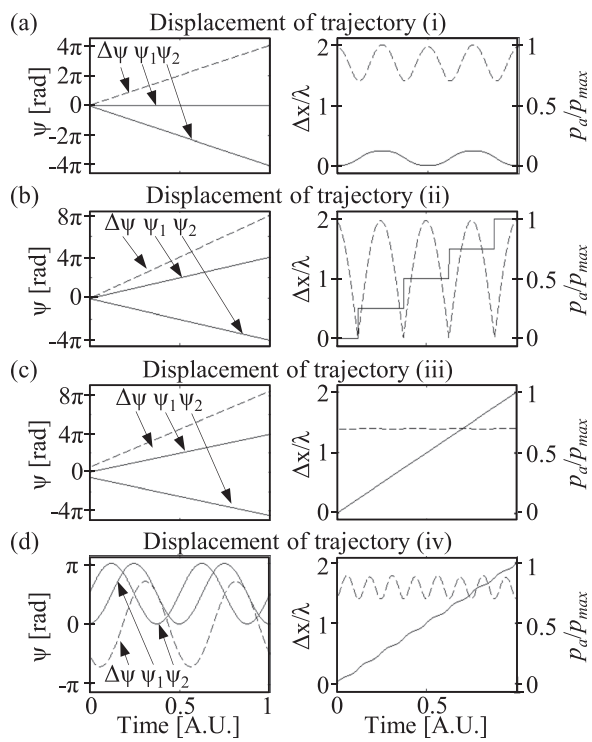

FIG. 5. Sequence of ψ_1, ψ_2 and $\Delta\psi = \psi_1 - \psi_2$ for trajectories (i)–(iv) (Fig. 2) in the left column, with the corresponding displacement of a particle trapped in a node (solid line), and the amplitude of the standing pressure wave (dashed line) in the right column. The pressure amplitude has been normalized with the maximum pressure amplitude, p_{max}, for the given reservoir dimensions and wave number.

This article is copyrighted as indicated in the article. Reuse of AIP content is subject to the terms at: http://scitation.aip.org/termsconditions. Downloaded to IP: 155.101.97.169 On: Fri, 15 May 2015 20:50:59

in $\Delta\psi$ is enabled by adjusting ψ_2 and maintaining ψ_1 constant. The node is displaced up to $\Delta x/\lambda = 1/4$, but further adjustment of ψ_2 results in no additional displacement. In Fig. 5(b) the linear change in $\Delta\psi$ is obtained by increasing ψ_1 and decreasing ψ_2 equally by $\Delta\psi/2$. While a displacement of multiple wavelengths appears to be obtained, the phase combinations where the step-wise displacements occur correspond to a standing pressure wave with zero amplitude, making controlled particle manipulation impossible. In Fig. 5(c), each phase is adjusted similarly to Fig. 5(b), with ψ_2 offset by an additional $\pi/2$, resulting in $\Delta\psi(0) \neq 0$. The nodal displacement is linear with respect to time, but the pressure amplitude, while almost constant, never reaches the maximum possible value. Finally, in Fig. 5(d), each phase is controlled independently along the trajectory shown in the inset of Fig. 2(a), and experimentally demonstrated in Fig. 4. This sequence of phases results in nodal displacements over multiple wavelengths, and the pressure amplitude is greater than or equal to that in the previous example. Note that the time scale of Fig. 4(a) seems different from that of Fig. 5(d). However, ψ_1 and ψ_2 follow the same sequence. Figure 5 shows that the values of ψ_1 and ψ_2 are more important than $\Delta\psi$, and that unconstrained manipulation of a particle trapped in a node cannot be achieved through linear adjustment of $\Delta\psi$, but can be realized through independent adjustment of ψ_1 and ψ_2. The pressure amplitude of the standing wave depends on ψ_1 and ψ_2, and displacement of a particle cannot occur if the amplitude of the standing pressure wave is zero. Although we performed this analysis for Eq. (7), the same methodology can be used for any $k \neq n\pi/L$ (Eq. (6)) to displace a particle over multiple wavelengths.

In conclusion, we have derived a theoretical model for the location of the nodes of a standing pressure wave generated by two opposing piezoelectric transducers with independent control of the transducer phases. A particle trapped in a node of the standing pressure wave can be precisely displaced over multiple wavelengths, by adjusting the phases of the transducers independently. As opposed to other methods in the literature, the theoretical model takes into account reflections normal to the transducer surface, removing the need for complicated experimental implementations with, e.g., matching layers, backing layers, or offset transducers. It is shown that when developing a sequence of transducer phases to achieve a specific displacement trajectory, special consideration must be given to the pressure amplitude of the standing wave. Using a simple experimental apparatus, it is demonstrated that a particle can be displaced over $\Delta x/\lambda = 2$, by applying a sequence of phase settings to both transducers. Good agreement between the theoretically predicted and experimentally measured displacement is observed.

[1]M. Evander and J. Nilsson, Lab Chip **12**, 4667 (2012).
[2]Y. Yamakoshi, Y. Koitabashi, N. Nakajima, and T. Miwa, Jpn. J. Appl. Phys., Part 1 **45**, 4712 (2006).
[3]Y. Yamakoshi, N. Nakajima, and T. Miwa, Jpn. J. Appl. Phys., Part 1 **46**, 4847 (2007).
[4]B. Raeymaekers, C. Pantea, and D. N. Sinha, J. Appl. Phys. **109**, 014317 (2011).
[5]J. Lee, K. Ha, and K. K. Shung, J. Acoust. Soc. Am. **117**, 3273 (2005).
[6]Y. Li, C. Lee, K. H. Lam, and K. K. Shung, Appl. Phys. Lett. **102**, 084102 (2013).
[7]J. Wu and G. Du, J. Acoust. Soc. Am. **87**, 997 (1990).
[8]K. Yosioka and Y. Kawasima, Acoustica **5**, 167 (1955).
[9]F. Zheng, Y. Li, H. Hsu, C. Liu, C. T. Chiu, C. Lee, H. H. Kim, and K. K. Shung, Appl. Phys. Lett. **101**, 214104 (2012).
[10]A. Grinenko, P. D. Wilcox, C. R. P. Courtney, and B. W. Drinkwater, Proc. R. Soc. London, Ser. A **468**, 3571 (2012).
[11]T. Kozuka, K. Yasui, A. Towata, and Y. Iida, Jpn. J. Appl. Phys., Part 1 **46**, 4948 (2007).
[12]C. R. P. Courtney, C.-K. Ong, B. W. Drinkwater, P. D. Wilcox, C. Demore, S. Cochran, P. Glynne-Jones, and M. Hill, J. Acoust. Soc. Am. **128**, EL195 (2010).
[13]C. R. P. Courtney, C. K. Ong, B. W. Drinkwater, A. L. Bernassau, P. D. Wilcox, and D. R. S. Cumming, Proc. R. Soc. London, Ser. A **468**, 337 (2011).
[14]A. Grinenko, C. K. Ong, C. R. P. Courtney, P. D. Wilcox, and B. W. Drinkwater, Appl. Phys. Lett. **101**, 233501 (2012).
[15]L. Kinsler, A. Frey, A. Coppens, and J. Sanders, *Fundamentals of Acoustics* (John Wiley and Sons Inc., New York, 2000).
[16]N. H. Asmar, *Partial Differential Equations and Boundary Value Problems with Fourier Series* (Pearson Prentice Hall, New Jersey, 2004), p. 173.
[17]J. E. Mark, *Polymer Data Handbook*, 2nd ed. (Oxford University Press, New York, 2009), p. 1036.

This article is copyrighted as indicated in the article. Reuse of AIP content is subject to the terms at: http://scitation.aip.org/termsconditions. Downloaded to IP: 155.101.97.169 On: Fri, 15 May 2015 20:50:59